V.I. KELEMEN, M.M. DOVHANYCH, E.YU. REMETA
Institute of Electron Physics, Nat. Acad. of Sci. of Ukraine
(21, Universytetska Str., Uzhgorod 88017; e-mail: vlad.kelemen@gmail.com, remetov@inbox.ru)

POTENTIAL ELECTRON SCATTERING BY PHOSPHORUS ATOM

PACS 34.80.Bm; 31.15.E-

Elastic scattering of electrons by phosphorus atoms within the collision energy range of 0.01–200 eV has been studied theoretically for the first time. The integral and differential cross sections are calculated in the spin-polarized approximation for a parameter-free real optical potential. The total and spin electron densities, the electrostatic potential, and the spin exchange and correlation-polarization potentials are found for the phosphorus atom in the local spin density approximation of the density functional theory. The features of the integral cross section at energies lower than 10 eV are studied in detail in various approximations and compared with the data for neighbor sulfur, chlorine, and argon atoms. The spin exchange asymmetry in the electron scattering by the phosphorus atom with a half-filled valence $3p^3$-subshell was studied with regard for the spin dependence of the exchange and polarization interactions.

Keywords: optical potential, spin-polarized, asymmetry, differential cross section, integral cross section, phase shift, partial cross section, critical minimum, Ramsauer–Townsend minimum.

1. Introduction

In the scattering of electrons by light atoms with unfilled valence $3p$-subshell, it is of a certain interest to reveal and to study the influence of a gradual filling of this subshell on the behavior of scattering parameters. It is also of importance to compare this behavior with the scattering data obtained for similar multielectron atoms. In this work, using the optical potential method, we calculate the cross-sections of elastic electron scattering by the phosphorus atom, the electron configuration of which in the ground state is $1s^2 2s^2 2p^6 3s^2 3p^3\ {}^4\mathrm{S}$. The cross-sections are compared with the corresponding calculated characteristics: the integral and differential cross-sections (DCSs) of electron scattering by the following atoms in the ground state: S ($3p^4\ {}^3\mathrm{P}$) [1, 2], Cl ($3p^5\ {}^2\mathrm{P}$) [3–5], and Ar ($3p^6\ {}^1\mathrm{S}$) [4]. For Ar atoms, we also give experimental data together with theoretical estimations [4, 6–8] and the results of calculations using our method. In works [1, 3], the calculations were carried out using the multiconfiguration Hartree–Fock method (from 109 to 170 configurations for the S atom and from 130 to 167 ones for the Cl atom) and omitting the relativistic effects. In work [2], the author used the nonrelativistic approximation of close coupling (27 states were taken into account) of the modified R-matrix method based on the B-spline representation of the scattering orbitals and taking their non-orthogonality into consideration. This method was used in work [5] in the semirelativistic Breit–Pauli approximation with pseudostates. In work [4], the nonrelativistic elastic and inelastic scatterings of electrons by argon and chlorine atoms were studied theoretically using the method of R-matrix with pseudostates (4 states for Ar and 17 states for Cl). Similarly to what was done in work [5], those pseudostates were introduced in [4] to consider the dipole polarization of the target electron shell. In work [6], the method of R-matrix was also used for calculations in the nonrelativistic

approximation. Such a comparison of calculation results is important in the cases where the experimental study of the particle scattering by chemically active atoms faces considerable difficulties. The results of comparison also clarify the theoretical reliability of calculated parameters.

Note that a similar comparison was theoretically considered earlier in work [9] using the atomic pairs (N, Ne) and (P, Ar) as examples. A nonrelativistic description with exact exchange interaction and model simulation of the polarization interaction was used.

Atomic systems with one half-filled subshell were described in the spin-polarized approximation [10,11], i.e. by accounting for the spin polarization of electron subshells. According to Hund's rule [10], the ground state of such systems has a maximum spin value, which is determined by the electrons in the half-filled subshell. The whole electron shell of an atom is divided into two filled spin subshells. In order to find the total and spin electron densities and the scattering potentials, we used the local spin density (LSD) approximation of the density functional theory (DFT) [11].

In the case of a spin-polarized atom, the exchange interaction of an incident electron characterized by a fixed spin direction is possible only with the corresponding spin subshell of the atom. Hence, the electron scattering by a phosphorus atom can be considered in the cases where the directions of the incident electron spin and the atom spin coincide (parallel-spin scattering) or are opposite (anti-parallel-spin scattering).

The spin of the system also affects the polarization interaction between the incident electron and the atom. In the interior region of the latter, the polarization interaction is governed by the correlation interaction of the incident electron with target electrons (see, e.g., works [12,13]). In the DFT, this interaction is described by a correlation functional, which, in the LSD approximation for the inhomogeneous spin-polarized electron gas, is determined by the correlation energy density. In work [14], the spin-dependent polarization potentials were found.

In this work, the scattering parameters are calculated using the method of real optical potential (OP). The results obtained for the parallel- and anti-parallel-spin scattering cross-sections make it possible to calculate the spin exchange asymmetry at the electron scattering [15] (see also works [14, 16]).

2. Theoretical Method

In the ground state of a phosphorus atom with the half-filled $3p^3$-subshell, the corresponding electron configuration has a maximum spin of $3/2$, i.e., according to Hund's rule, the electrons in this subshell have identically directed spins. This allows us to divide the whole electron shell of the atom into two filled spin shells: nine electrons with the spins conditionally directed upward ($sp = \uparrow$) and six electrons with the spins directed downward ($sp = \downarrow$). From the atomic calculation, we obtain two spin, $\rho_\uparrow(r)$ and $\rho_\downarrow(r)$, and total, $\rho(r) = \rho_\uparrow(r) + \rho_\downarrow(r)$, electron densities.

Electron scattering by a phosphorus atom can be considered in two cases: where the spin directions of the incident electron and the atom coincide (parallel-spin scattering, $\uparrow\uparrow$, the total spin of the system equals 2) and where they are directed oppositely (anti-parallel-spin scattering, $\downarrow\uparrow$, the total spin of the system equals 1). In those cases, the scattering of electron by such a spin-polarized atom is described by two real spin optical potentials ($\lambda = \uparrow\uparrow, \downarrow\uparrow$):

$$V^\lambda_{\rm opt}(r,E) = V_{\rm S}(r) + V^\lambda_{\rm ex}(r,E) + V^\lambda_{\rm pol}(r) + \\ + V_{\rm R}(r,E) + V^\pm_{\rm so}(r). \qquad (1)$$

The spin-dependent potential $V^\lambda_{\rm opt}(r,E)$ is a sum of the following interaction potentials: static $V_{\rm S}(r)$, spin exchange $V^\lambda_{\rm ex}(r,E)$, spin polarization $V^\lambda_{\rm pol}(r)$, relativistic $V_{\rm R}(r,E)$ and the potential of spin-orbit interaction $V^\pm_{\rm so}(r,E)$. The potential $V_{\rm R}(r,E)$ looks like (see works [17–19]):

$$V_{\rm R}(r,E) = -\frac{\alpha^2}{2}V_{\rm S}^2 + \frac{\chi}{4}\frac{d^2V_{\rm S}}{dr^2} + \frac{3\chi^2}{8}\left(\frac{dV_{\rm S}}{dr}\right)^2, \qquad (2)$$

where $\chi = \alpha^2/[2 + \alpha^2(E - V_{\rm S})]$, and α is the fine-structure constant. The superscript $\pm$ in Eq. (1) corresponds to the magnitude of the total angular momentum of the electron, $j = \ell \pm 1/2$, where ℓ is the orbital momentum of an electron. In expressions (1) and (2), E is the energy of the incident electron (the atomic system of units is used: $e = m_e = \hbar = 1$).

Below, following our previous works (see, e.g., works [17, 20–22] and references therein), the calculation with the application of the real potentials (1) will be called the RSEP approximation, and the calculation using potential (1) but without the component $V_{\rm R}(r,E)$, the SEPSo approximation.

The static potential $V_{\rm S}(r)$ and the electron densities $\rho(r)$ and $\rho_{\rm sp}(r)$ were calculated numerically

in the framework of a self-consistent atomic scheme and the scalar-relativistic and LSD approximations of the DFT with the exclusion of the electron self-action energy (see, work [23] and references therein). Those quantities were approximated by analytical expressions taken from work [24] (see Eqs. (A1) and (A2), as well as the corresponding parameters, in Appendix). The potential of spin-orbit interaction $V_{\rm so}^{\pm}(r)$ ($\sim dV_{\rm S}(r)/dr$) was used in the form of expression (5) taken from work [17] (see also work [25] and references therein).

The exchange interaction was taken into account in the framework of the free electron gas approximation (see work [23]). Two values of Fermi momentum $k_{\rm F}^{sp}(r) = [6\pi^2\rho_{\rm sp}(r)]^{1/3}$ used in the spin-polarized scattering approximation gave two exchange potentials $V_{\rm ex}^{\lambda}(r,E)$: $V_{\rm ex}^{\uparrow\uparrow}$ for $k_{\rm F}^{\uparrow}$ and $V_{\rm ex}^{\downarrow\uparrow}$ for $k_{\rm F}^{\downarrow}$. The value of the ionization potential for a phosphorus atom, $I = 10.4992$ eV, which is a parameter of the exchange potential, was obtained in the same approximation as the static potential $V_{\rm S}$.

The polarization potential consists of two parts determined at short (short-range, SR) and long (long-range, LR) distances,

$$V_{\rm pol}^{\lambda}(r) = \begin{cases} Vp_{\lambda}^{\rm SR}(r), & r \le r_c^{\lambda} \\ Vp^{\rm LR}(r), & r > r_c^{\lambda}, \end{cases} \qquad (3)$$

where r_c^{λ} is the coordinate of the intersection point (see below). As was noted above, the potential $V_{\rm pol}^{\lambda}(r)$ in the inner atomic region is governed by the correlation interaction between the incident electron and the target electrons. In the LSD approximation of the DFT, the functional of this interaction looks like

$$E_c^{\rm LSD}[\rho_{\uparrow},\rho_{\downarrow}] = \int d\mathbf{r}\rho(\mathbf{r})\varepsilon_c[\rho_{\uparrow}(\mathbf{r}),\rho_{\downarrow}(\mathbf{r})]. \qquad (4)$$

The energy density $\varepsilon_c[\rho_{\uparrow}(r),\rho_{\downarrow}(r)] \equiv \varepsilon_c[r_s(r),\zeta(r)]$ depends on the spin polarization function $\zeta(r) = [\rho_{\uparrow}(r) - \rho_{\downarrow}(r)]/\rho(r)$ and the Wigner radius $r_s(r) = \{3/[4\pi\rho(r)]\}^{1/3}$, and it can be calculated by applying formulas from work [14].

At distances $r \le r_c^{\lambda}$, the polarization potential obtained from Eq. (4) using the variation technique looks like [14, 16]:

$$Vp_{\lambda}^{\rm SR}(r) = \varepsilon_c(r_s,\zeta) - \frac{r_s}{3}\frac{d\varepsilon_c}{dr_s} \pm (1 \mp \zeta)\frac{\partial\varepsilon_c}{\partial\zeta}. \qquad (5)$$

In Eq. (5), the upper signs correspond to the case $\lambda = \uparrow\uparrow$, and the lower ones to $\lambda = \downarrow\uparrow$. The derivatives $d\varepsilon_c/dr_s$ and $\partial\varepsilon_c/\partial\zeta$ were calculated in work [14] (see also Appendix B in work [16]).

At distances $r > r_c^{\lambda}$, the polarization potential has the well-known asymptotic limit $Vp^{\rm LR}(r) = -\alpha_d(0)/2r^4$, where $\alpha_d(0)$ is the static dipole polarizability. The two parts of polarization potential, $Vp_{\lambda}^{\rm SR}(r)$ and $Vp^{\rm LR}(r)$, intersect at $r_c^{\uparrow\uparrow} = 6.456a_0$ for the parallel-spin scattering, $\lambda = \uparrow\uparrow$, and at $r_c^{\downarrow\uparrow} = 3.980a_0$ for the anti-parallel-spin one (here, a_0 is the atomic length unit equal to the first Bohr radius of a hydrogen atom). The polarizability of a phosphorus atom, $\alpha_d(0) = 30.65a_0^3$, was calculated in the local approximation of the time-dependent DFT [23, 26] with an effective relativistic local potential (see works [22, 27] and references therein).

Note that, in works [14, 16, 28], it was shown for a number of atoms taken as an example that, while calculating the asymmetry of the electron scattering by an atom with half-filled valence subshell, it is not enough to consider the spin dependence of only the exchange interaction; the spin dependence of the polarization interaction should be taken into account as well.

At calculations of the scattering cross-sections in a wide interval of energies, we may use the averaged optical potential:

$$V_{\rm opt}^{\rm av}(r,E) = V_{\rm S}(r) + V_{\rm ex}^{\rm av}(r,E) + V_{\rm pol}^{\rm av}(r) + \\ + V_{\rm R}(r,E) + V_{\rm so}^{\pm}(r), \qquad (6)$$

where $V_{\rm ex}^{\rm av} = (V_{\rm ex}^{\uparrow\uparrow} + V_{\rm ex}^{\downarrow\uparrow})/2$, and the potential $V_{\rm pol}^{\rm av}$ has the averaged short-range component $Vp_{av}^{\rm SR} = (Vp_{\uparrow\uparrow}^{\rm SR} + Vp_{\downarrow\uparrow}^{\rm SR})/2$. It is convenient to use the averaged optical potential in cumbersome calculations, while determining the critical minima in DCSs and the points of total spin polarization of scattered electrons.

As a result of calculations with the potentials $V_{\rm opt}^{\lambda}(r,E)$ (see Eq. (1)), we obtain four sets of partial real phase shifts $\delta_{\ell}^{\lambda,\pm}(E)$. Similarly to what was done in our previous works [20–23, 25, 27–30], in order to calculate the phases shifts, we use the method of phase functions [31, 32]. The procedure of numerical solution of the phase equations was described in works [20–23, 25]. Knowing the phase shifts $\delta_{\ell}^{\lambda,\pm}$, we can find "the direct" scattering amplitudes,

$$f^{\lambda}(E,\theta) = \frac{1}{2ik}\sum_{\ell=0}^{\infty}\Big\{(\ell+1)[\exp(2i\delta_{\ell}^{\lambda,+}) - 1] + \\ + \ell[\exp(2i\delta_{\ell}^{\lambda,-}) - 1]\Big\}P_{\ell}(\cos\theta) \qquad (7)$$

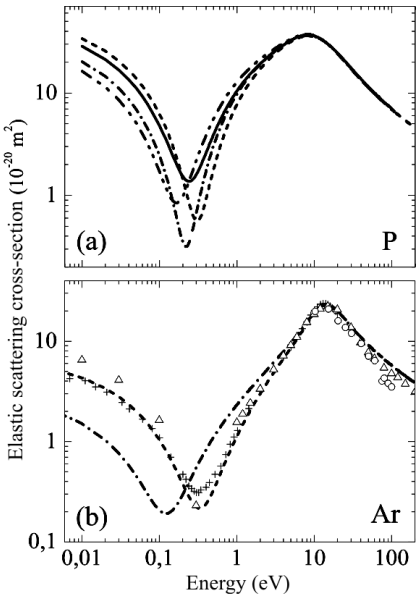

Fig. 1. Energy dependences of the elastic electron scattering cross-section for (a) phosphorus and (b) argon atoms. Relativistic RSEP approximation: spin-polarized approach (SPA) (solid curves) and spin-unpolarized approach (LA) (dashed curves). The account for the spin-orbit interaction in the SEPSo approximation: SPA approach (dot-dot-dashed curves) and LA approach (dot-dashed curves). Experimental data: crosses [7], triangles [33], and circles [34]

and the "spin-flip" scattering amplitudes

$$g^{\lambda}(E,\theta) = \frac{1}{2ik}\sum_{\ell=1}^{\infty}[\exp(2i\delta_{\ell}^{\lambda,-}) - \\ - \exp(2i\delta_{\ell}^{\lambda,+})]P_{\ell}^{1}(\cos\theta), \quad (8)$$

where θ is the scattering angle, $k = (2E)^{1/2}$ is the momentum of the incident electron, $P_{\ell}(\cos\theta)$ are the Legendre polynomials, and $P_{\ell}^{1}(\cos\theta)$ are the associated Legendre functions of the first kind. The differential cross-sections of parallel-spin, $d\sigma^{\uparrow\uparrow}/d\theta$, and anti-parallel-spin, $d\sigma^{\downarrow\uparrow}/d\theta$, elastic scatterings can be determined using those amplitudes by the formula

$$\frac{d\sigma^{\lambda}(E,\theta)}{d\theta} = |f^{\lambda}(E,\theta)|^2 + |g^{\lambda}(E,\theta)|^2. \quad (9)$$

The angular dependence of the spin exchange asymmetry function $A(E,\theta)$ at the elastic scattering is calculated using the expression

$$A(E,\theta) = \\ = (d\sigma^{\downarrow\uparrow}/d\theta - d\sigma^{\uparrow\uparrow}/d\theta)/(d\sigma^{\downarrow\uparrow}/d\theta + d\sigma^{\uparrow\uparrow}/d\theta). \quad (10)$$

The averaged differential cross-section of elastic scattering can be found by the formula

$$\frac{d\sigma}{d\theta} = \frac{1}{2}\left(\frac{d\sigma^{\uparrow\uparrow}}{d\theta} + \frac{d\sigma^{\downarrow\uparrow}}{d\theta}\right). \quad (11)$$

The integral elastic, $\sigma_{\rm el}$, momentum-transfer, $\sigma_{\rm mom}$, and viscosity, $\sigma_{\rm vis}$, scattering cross-sections, which are of importance for applications to plasma physics, are determined according to the general formula as the averages of spin cross-sections

$$\sigma(E) = (\sigma^{\uparrow\uparrow}(E) + \sigma^{\downarrow\uparrow}(E))/2. \quad (12)$$

At calculations of the integral spin cross-sections, expressions from work [14] were used.

3. Discussion of Results

In Figs. 1 to 3, the integral cross-sections for the potential scattering of an electron by the phosphorus atom calculated in the semirelativistic (SEPSo) and relativistic (RSEP) approximations with the use of the local spin-unpolarized (LA) and spin-polarized (SPA) approaches are depicted. The results are compared with the data for the argon obtained experimentally [7, 8, 33, 34] and calculated by us in the RSEP and SEPSo approximations. Our results are quite consistent with the data of work [9] – for the atom of phosphorus, it is of quality, and for atom of argon both qualitative and quantitative

The behavior of the cross-sections in all three figures is similar: they have a deep minimum and rather a high maximum, which qualitatively coincides with experimental data obtained for the cross-sections of scattering by the argon atom [7, 8, 33, 34]. Note that the cited cross-sections for the argon are well described by the results of our calculations in the RSEP approximation. Neglecting the potential $V_{\rm R}(r,E)$ (Eq. (2)) in the SEPSo approximation results in a shift of the minima toward lower energies and in the smaller cross-section values for near-threshold energies (see panels b in Figs. 1–3). It is evident that, although the phosphorus and argon atoms are light, the relativistic effects are rather substantial. In the case of a phosphorus atom, this influence exists for both approximations, spin-polarized and spin-unpolarized (rougher) ones (see panels a in Figs. 1–3). At the energies of cross-section maxima –

10 eV for elastic, 6 eV for momentum-transfer, and 4 eV for viscosity cross-sections – the indicated effects and the difference in the local description do not affect the behavior of parameters any more. For the phosphorus atom, the behavior and the magnitude of elastic cross-section at energies below 10 eV are mainly driven by the cross-section of anti-parallel-spin scattering.

The behavior of the integral cross-sections for the elastic and momentum-transfer scattering in the case of a phosphorus atom is similar to that for sulfur [1] and chlorine [3] atoms. The total cross-section is mainly composed of the quartet cross-section [1] in the case of an S atom and of the triplet one in the case of Cl atom [3].

In work [2], the cross-section of elastic electron scattering by the sulfur atom was calculated using the approximations with 3, 15, and 27 expansion states in the close coupling model of a modified R-matrix method. The obtained behavior of the cross-section in all cases was similar to that at the scattering by P, S, and Cl atoms. The first approximation differs considerably from the second and the third one in the whole interval of collision energy—from the threshold up to 40 eV. Those two approximations yield results close to each other; however, in the near-threshold energy region (lower than 1.5 eV), the approximation that involves 27 states is the best: is gives a deeper minimum, which is located at a lower energy. This fact testifies to the importance of the effects of the atomic electron shell polarization by the incident electron.

The energy of the cross-section minimum in the case of elastic electron scattering by a chlorine atom, which was determined in work [5], has a small value of about 0.2 eV. It is rather sensitive to the model used in a theoretical description of the scattering. This especially concerns the descriptions of the target atom structure. The minimum in the cross-section mentioned above emerges only if the polarization interaction is considered. In work [5], the cross-section at a very low energy of 0.001 eV equals about 7×10^{-20} m^2, which is slightly larger than the cross-section at 0.01 eV (see Table) and much smaller that the cross-sections calculated in works [3, 4]. The behavior of the integral momentum-transfer cross-section $\sigma_{\rm mom}$ is similar to the elastic one: it has the minimum $\sigma_{\rm mom} \approx 1.25 \times 10^{-20}$ m^2 at 0.1 eV and the maximum $\sigma_{\rm mom} = 15.6 \times 10^{-20}$ m^2 at 10 eV. At low ener-

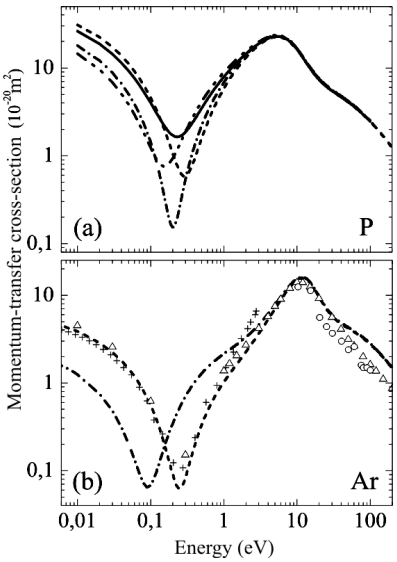

Fig. 2. Energy dependences of the momentum-transfer cross-section at elastic electron scattering by (a) phosphorus and (b) argon atoms. Relativistic RSEP approximation: SPA approach (solid curves) and LA approach (dashed curves). SEPSo approximation: SPA approach (dot-dot-dashed curves) and LA approach (dot-dashed curves). Experimental data: crosses [8], triangles [33], and circles [34]

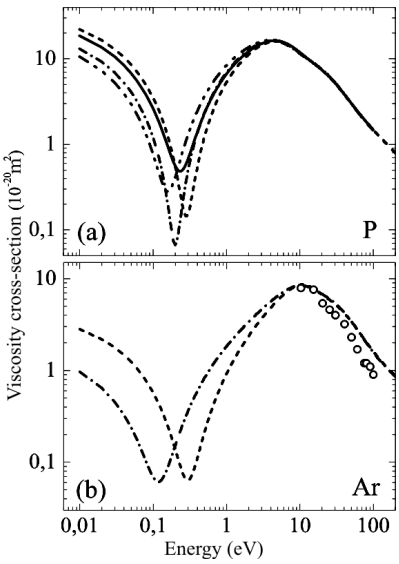

Fig. 3. Energy dependences of the viscosity cross-section at elastic electron scattering by (a) phosphorus and (b) argon atoms. Relativistic RSEP approximation: SPA approach (solid curves) and LA approach (dashed curves). The SEPSo approximation: SPA approach (dot-dot-dashed curves) and LA approach (dot-dashed curves). Experimental data: circles [34]

Parameters of the features in the integral cross-section of elastic electron scattering by P, S, Cl, and Ar atoms

Method	a, a_0	σ (0.01 eV), 10^{-20} m^2	$E_{\rm RT}$, eV	$\sigma_{\rm RT}$, 10^{-20} m^2	$E_{\max}$, eV	$\sigma_{\max}$, 10^{-20} m^2
			P($3p^3$)			
RSEP_LSA	(p) –3.380 (a) –3.621	28.541	0.24	1.3715	8.2	36.976
RSEP_LA	–3.780	33.867	0.31	0.5591	8.45	36.079
SEPSo_LSA	(p) –2.745 (a) –2.750	16.318	0.17	0.8467	7.98	37.253
SEPSo_LA	–3.007	20.156	0.22	0.3163	8.2	36.313
			S($3p^4$)			
[1]	(q) –4.2558 (d) –1.6273	∼30	0.475	5.4439	8.50	30
[2]	–	∼40	∼0.5	∼5	∼8.4	∼25
			Cl($3p^5$)			
[3]	(t) –2.7072 (s) –1.4778	>30	0.9524	2.4483	10.20	30
[4]	–	∼25	∼0.7	∼2.1	11	26
[5]	(t) –1.495 (s) –1.035	5	≈0.2	2.5	∼13	23.2
			Ar($3p^6$)			
RSEP_LA	–1.308	4.309	0.33	0.2157	14.5	22.995
[7]	–1.365	4.04	0.3	0.31	13.02	23.80
[33]	–	6.5	0.3	0.23	15	22
[4]	–	2.5(∼0.04 eV)	∼0.27	∼0.3	∼22.5	13.75
[34]	–	–	–	–	15.3	21
[40]	–	–	–	–	15	22.28
[6]	–	–	–	–	14	23.661

N o t a t i o n: p (parallel), a (anti-parallel), q (quartet), d (doublet), t (triplet), s (singlet).

gies, it equals $\sigma_{\rm mom}(0.001\ {\rm eV}) = 3.75\times10^{-20}$ m^2 and $\sigma_{\rm mom}(0.01\ {\rm eV}) \approx 6\times10^{-20}$ m^2, which is also much smaller than the values obtained in works [3, 4].

The energy of the elastic cross-section minimum for the electron scattering by a chlorine atom (about 0.7 eV) obtained in work [4] is rather substantial. The energy of the same minimum but for the electron scattering by an argon atom [4] has a smaller value of about 0.27 eV. Those parameters are rather sensitive to the number of pseudostates that were taken into account in calculations and associated with the description of the polarization interaction at the scattering. The behavior of the integral momentum-transfer cross-sections $\sigma_{\rm mom}$ is similar to that of the elastic cross-sections: for a Cl atom, a minimum of 1.8×10^{-20} m^2 at 0.7 eV and a maximum of 18×10^{-20} m^2 at 9 eV; for an Ar atom, a minimum of 0.2×10^{-20} m^2 at 0.3 eV and a maximum of 16×10^{-20} m^2 at 11.25 eV. At low energies, it equals $\sigma_{\rm mom}(\sim 0\ {\rm eV}) \approx 0.5\times10^{-20}$ m^2. The cross-sections $\sigma_{\rm mom}$ and $\sigma_{\rm vis}$ at an energy of 0.001 eV calculated by us in the RSEP approximation equal 5.7×10^{-20} m^2 (2.3×10^{-20} m^2 in the SEPSo approximation) and 3.9×10^{-20} m^2 (1.6×10^{-20} m^2 in the SEPSo approximation), respectively. In work [8], the dependence $\sigma_{\rm mom}(E)$ was obtained with the use of experimen-

tal data from work [7]. In particular, the cross-section $\sigma_{\rm mom} = 4.7 \times 10^{-20}$ m^2 at an energy of 0.003 eV. This value is close to ours. Hence, the influence of relativistic effects is rather considerable; therefore, the nonrelativistic cross-sections in work [4] are small.

The minimum of the elastic cross-section $\sigma_{e\ell}$ at low energies, which was obtained for the examined atoms, is the so-called Ramsauer–Townsend (RT) minimum located at $k_{\rm RT} = (2E_{\rm RT})^{1/2} = -3a/(\pi\alpha_d(0))$ [35]. It stems from the mutual action of the exchange and polarization potentials of electron–atom interaction and reflects a reduction of the phase shift of the s-wave at higher energies if the scattering length a is negative: $\delta_0(k) \approx 3\pi - ak - \pi\alpha_d(0)k^2/3$. The multiplicity factor π originates from the presence of three filled s-subshells in the atoms belonging to the third period in the Periodic table of elements. For a phosphorus atom, the minimum in the s-wave partial cross-section equals $\sigma_0 = 2.41 \times 10^{-20}$ m^2 at 0.31 eV. The maximum of $\sigma_{e\ell}$ is formed, first of all, by the contributions of the p- and d-wave partial cross-sections (of about 79%).

The peculiarities in the cross-section parameters calculated for the elastic electron scattering by related atoms P, S, Cl, and Ar using various methods are compared in Table. These are the scattering length a, near-threshold cross-sections $\sigma(0.01$ eV), energies $E_{\rm RT}$ and cross-sections $\sigma_{\rm RT}$ at the Ramsauer–Townsend minimum, and the energies $E_{\max}$ and cross-sections $\sigma_{\max}$ at the maximum. One can see that, in the case of Ar, the near-threshold cross-section $\sigma(0.01$ eV) is almost 7 times as small as the cross-sections for other atoms, and $\sigma_{\rm RT}$ and $\sigma_{\max}$ are the smallest. Note that the static dipole polarizabilities for P, S, Cl, and Ar atoms decrease with the growth of the nucleus charge and equal (in terms of a_0^3) 24.93, 19.37, 14.57, and 11.07, respectively [36] (see also work [37]). The same tendency was also observed in our calculations for $\alpha_d(0)$. Note that, in general, the behavior and the magnitude of cross-sections are formed by the scattering with a large total spin. In particular, the total cross-section mainly consists of the quartet cross-section [1] in the case of an S atom and of the triplet one in the case of a Cl atom [3].

The scattering length is negative for all atoms, being maximal by the absolute value for an S atom and minimal for an Ar one. Note that, in work [38], the experimental scattering length obtained for an Ar atom amounted to $a = -1.492a_0$, whereas the

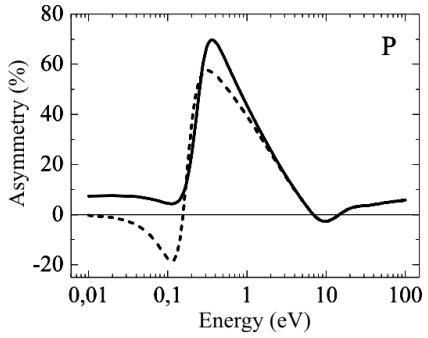

Fig. 4. Energy dependences of the spin exchange asymmetry function (13) at elastic electron scattering by a phosphorus atom. Calculations in the spin-polarized approach (SPA): RSEP approximation (solid curve) and SEPSo approximation (dashed curve)

theoretical calculation [39] using the phase equation from work [31, 32] and a model pseudo-potential gave $a = -1.512a_0$ (other data concerning the scattering length can also be found in the cited works). The cited values are close to more modern data [7] and the results of our RSEP calculations (see also work [8]), which are quoted in Table. In the case of a chlorine atom, the semirelativistic values of scattering length from work [5] ($-1.541a_0$ for the triplet, t, and $-0.857a_0$ for the singlet, s) are a little different from their nonrelativistic counterparts [3] also quoted in Table.

Of certain general interest is the behavior of the energy dependence of the asymmetry calculated with the use of the integral spin cross-sections of elastic scattering,

$$A_{e\ell}(E) = (\sigma_{e\ell}^{\downarrow\uparrow} - \sigma_{e\ell}^{\uparrow\uparrow})/(\sigma_{e\ell}^{\downarrow\uparrow} + \sigma_{e\ell}^{\uparrow\uparrow}). \qquad (13)$$

In Fig. 4, the results of calculations of those dependences in the RSEP and SEPSo approximations are depicted. One can see that the account for relativistic effects makes a substantial influence on the asymmetry at low (less than 1 eV) energies. At energies in a vicinity of the Ramsauer–Townsend minimum, the scattering asymmetry is maximal and equal to about 70%. In the near-threshold region and at energies higher than 10 eV, the asymmetry is less than 10%. The general behavior of the asymmetry is similar to the energy dependence for an antimony atom [28], which was calculated in the SEPSo approximation: the asymmetry has a maximum of about 70% at 0.19 eV, and its value does not exceed 10% at en-

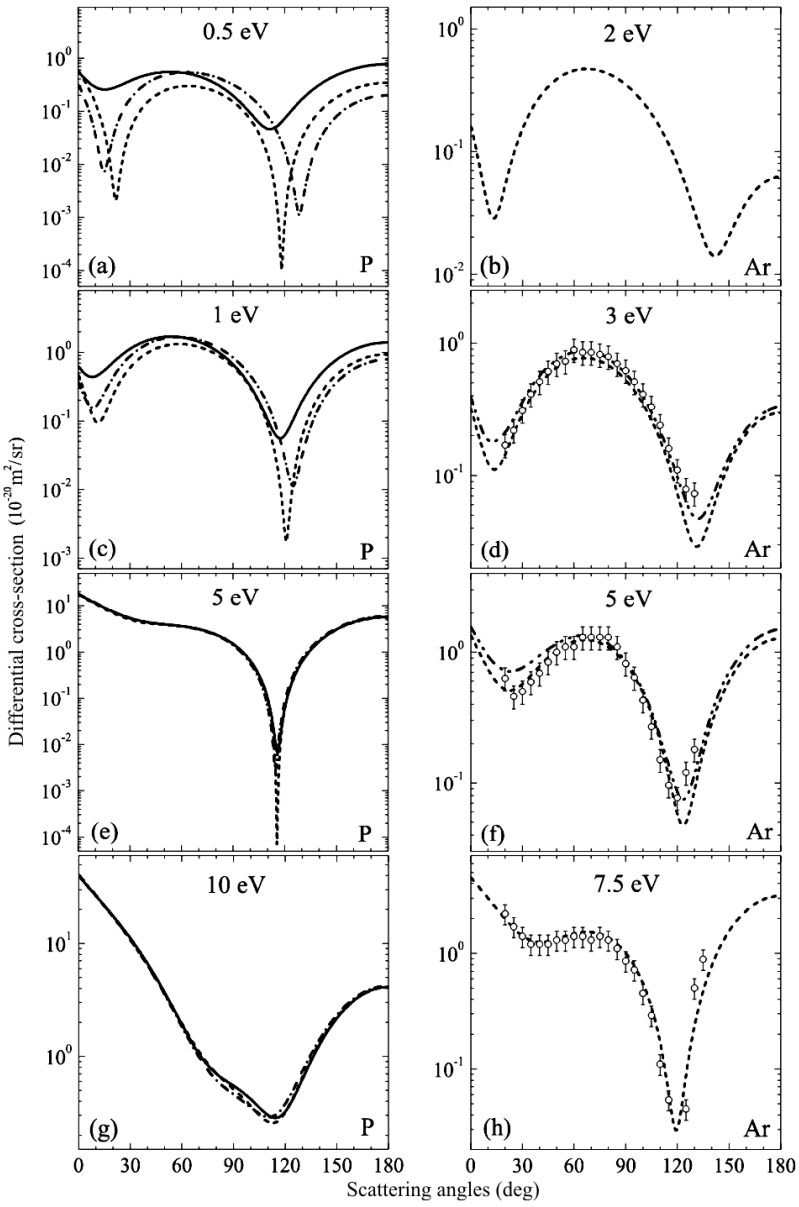

Fig. 5. Angular dependences of differential cross-sections for elastic electron scattering by phosphorus (panels *a*, *c*, *e*, and *g*) and argon (panels *b*, *d*, *f*, and *h*) atoms at collision energies E: for the phosphorus atom, $E = 0.5$ (*a*), 1 (*c*), 5 (*e*), and 10 eV (*g*); for the argon atom, $E = 2$ (*b*), 3 (*d*), 5 (*f*), and 7.5 eV (*h*). Relativistic RSEP approximation: SPA approach (solid curves) and LA approach (dashed curves). The SEPSo approximation and LA approach (dot-dashed curves). Nonrelativistic R-matrix calculation for the argon atom [6] (dot-dot-dashed curve). Experimental data: circles [40]

ergies from 10 to 200 eV. Hence, it is important to apply the spin-polarized approximation in a wide interval of collision energies: from the threshold value to several hundreds electronvolts.

In Fig. 5, the DCSs of elastic electron scattering by a phosphorus atom calculated in the approximations mentioned above for a number of low scattering energies (0.5, 1, 5, and 10 eV) are depicted. For the

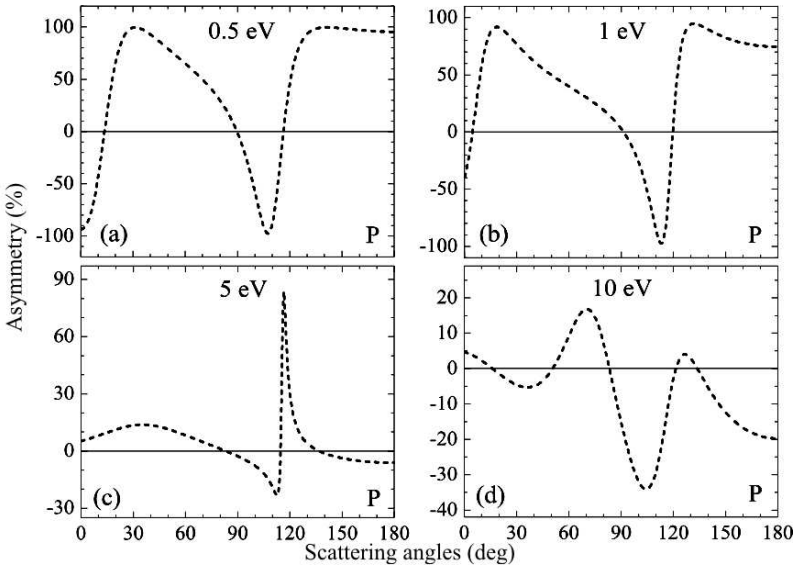

Fig. 6. Angular dependences of the spin exchange asymmetry function (10) for elastic electron scattering by a phosphorus atom calculated in the spin-polarized RSEP approximation for collision energies of 0.5 (*a*), 1 (*b*), 5 (*c*), and 10 eV (*d*)

sake of comparison, the DCS-results for elastic electron scattering by an argon atom are also shown: the results calculated by us at energies of 2, 3, 5, and 7.5 eV in the RSEP approximation, experimental results [40], and the results of R-matrix calculations [6]. At all energies, the DCS behavior for phosphorus qualitatively does not depend on the approximation type. Only the DCS magnitude substantially depends on the approximation, which manifests itself the most pronouncedly in the minima. For energies of 0.5 and 1 eV, the DCS has two minima at about 10–12° and 111–118°, with the role of relativistic effects and the spin polarization still remaining considerable (Fig. 5, panels *a* to *c*).

One can see that, starting from an energy of 5 eV, the DCSs calculated in the indicated approximations coincide at all angles (Fig. 5, *e*). At an energy of 5 eV, they differ by value only in a narrow angular vicinity of the DCS minimum at about 116°. This minimum is located in a narrow vicinity of the so-called critical minimum. Note that, in our work [25], a similar critical DCS minimum in the case of argon atom was predicted in the SEPSo approximation at an energy of 8.44 eV and an angle of 119.89°. The energy and the angular positions of such minima are sensitive to the accuracy of used approximations. For instance, the RSEP calculation for a phosphorus atom in the spin-polarized approximation with the averaged potential $V_{\rm opt}^{\rm av}(r, E)$ (Eq. (6)) gave the parameters of this critical minimum $E = 4.54$ eB and $\theta = 116.49°$, and in the spin-unpolarized approximation, $E = 5.02$ eV and $\theta = 115.57°$. The DCS magnitudes at those minima equal 4.9×10^{-25} m^2/sr and 4.3×10^{-25} m^2/sr, respectively (see also Fig. 5, *e*).

As the energy increases to 10 eV, the DCS minimum remains to stay in a vicinity of 115°, but it becomes wider and shallower. We would like to emphasize that this high-angle minimum is present in all DCS dependences (see also the cross-sections for argon in Fig. 5).

In general, the behavior and the magnitude of DCS for a phosphorus atom are governed by the behavior and the magnitude of the anti-parallel-spin scattering cross-section. At low energies, in particular, 0.5 and 1 eV, the DCS magnitude for forward (0°) scattering is determined by the cross-section of parallel-spin scattering. Note also that, at those energies, the cross-section magnitude for scattering at small angles (close to 0°) is smaller than the DCS values at medium angles (see Fig. 5, panels *a* and *c*). A similar relationship between DCS values was observed for the scattering by argon atoms at energies of 2 and 3 eV (see the theoretical and experimental data in Fig. 5, panels *b* and *d*). The calculations showed that, at the

indicated energies, the form of the angular DCS dependence is determined exclusively by the behavior of the real part of the direct scattering amplitude Re $f(E,\theta)$. In particular, the presence of a low-angle minimum in the DCS at about 10° is a consequence of the interference of many (more than 10) partial waves, as well as a non-trivial low-energy dependence of the s- and p-partial-wave phase shifts. Similar reasoning is also valid for the scattering by a phosphorus atom.

In works [1, 3], the DCSs for the electron scattering by sulfur and chlorine atoms with the unfilled valence $3p$-subshell were calculated for four energies: 0.001, 0.01, 0.1, and 1 Ry (1 Ry = 13.6058 eV). The angular dependences of the DCS for the scattering by those atoms turned out to be qualitatively similar: flat and structureless, especially at energies of 0.1 and 1 Ry. They are determined by the DCS for the system with a large total spin: 3/2 (quartet) in the S case and 1 (triplet) in the Cl one.

A comparison of our cross-section values with the data for sulfur and chlorine atoms demonstrates that, at small (less than 30°) angles and energies less than 5 eV, the scattering DCSs for the phosphorus are smaller by an order of magnitude. Moreover, the DCSs for S and Cl have no peculiar behavior with a minimum in a vicinity of 115°, as is observed in the case of phosphorus atom. However, at 10 eV, the angular dependences of the DCSs for P, S, and Cl atoms are very similar qualitatively and almost quantitatively.

The study of the angular dependence of the spin exchange asymmetry function $A(E,\theta)$ (see Eq. (10)) at electron scattering by phosphorus atoms is also important. In Fig. 6, the dependences $A(E,\theta)$ are plotted for the same energies of 0.5, 1, 5, and 10 eV as for the DCSs in Fig. 5. They are characterized by an essentially nonmonotonous behavior and almost reach the maximum value (100%) at definite angles for energies of 0.5, 1, and 5 eV (Fig. 6, panels a to c). The features obtained at 0.5 and 1 eV correspond to different manifestations of the spin dependence of the exchange and polarization interactions at anti-parallel- or parallel-spin electron scattering (see works [14,16]).

The function $A(E,\theta)$ has a very sharp maximum of 83.6% at the energy $E = 5$ eV and the angle $\theta = 116.5°$. At this angle, the DCS for parallel-spin scattering has a deep minimum, $d\sigma^{\uparrow\uparrow}/d\theta = 1.4 \times 10^{-23}$ m^2/sr, whereas for anti-parallel-spin one, $d\sigma^{\downarrow\uparrow}/d\theta = 1.5 \times 10^{-22}$ m^2/sr or is smaller by more than an order of magnitude. As a result, the asymmetry function (10) acquires a large positive value. It was noted above that, at an energy of 5 eV, the DCSs calculated in various approximations coincide at all angles, being different by magnitude only in a narrow angular vicinity of the critical minimum at about 116° (see Fig. 5, e). The spin DCSs are also close to one another at 5 eV. For example, the anti-parallel-spin scattering cross-section has a deep minimum at 115°, where $d\sigma^{\downarrow\uparrow}/d\theta = 9.85 \times 10^{-23}$ m^2/sr. Hence, the difference between the angular positions of spin DCS minima comprises only 1.5°. Accordingly, the function $A(E,\theta)$ acquires a sharp nonmonotonous behavior of the minimum-maximum type in a narrow interval of angles 110–120° (see Fig. 6, c).

As the energy of incident electron increases, the asymmetry decreases. For instance, the asymmetry is much smaller by value at 10 eV than at low energies (Fig. 6, d). The angular profile of the function $A(E,\theta)$ at 10 eV (two minima and two maxima, the magnitudes of which fall within the interval from 17 to 35%) is similar to the corresponding behavior of the asymmetry parameter for an antimony atom [14, 28].

4. Conclusions

Potential scattering of an electron by a phosphorus atom at collision energies of 0.01–200 eV was considered theoretically in the semirelativistic and relativistic approximations in the framework of the optical potential method and using the local spin-unpolarized and spin-polarized approaches. Peculiarities in the integral elastic scattering cross-section typical of the near-threshold scattering – a Ramsauer–Townsend minimum associated with the action of the attractive polarization interaction and followed by a maximum – were revealed. The parameters of elastic scattering (the scattering length, the minimum and maximum energies, and the corresponding cross-section values) were compared with the results of calculations carried out using various methods for the electron scattering by the neighbor (in the Periodic table) sulfur, chlorine, and argon atoms. The peculiarities obtained for the elastic cross-section were reproduced in the integral momentum-transfer and viscosity cross-sections.

At certain collision energies, the angular dependence of the differential cross-sections of electron

scattering by a phosphorus atom was found to have a few narrow minima similar to those, which are inherent to the cross-section of electron scattering by an argon atom. In the low-energy interval (below 10 eV), the energy and the angular position of the critical minimum were determined. The characteristics of such minima were demonstrated to depend on the approximation choice. Similar minima in the differential cross-sections of electron scattering by sulfur and chlorine atoms have not been studied earlier. The magnitudes of forward differential cross-section for the electron scattering by phosphorus and argon atoms at low collision energies were found to be smaller than the corresponding values obtained at medium angles.

The energy dependence of the spin exchange asymmetry is nonmonotonous and has a positive maximum. As the collision energy increases, the asymmetry decreases by value. The energy dependences of the asymmetry for phosphorus and antimony atoms are similar. The angular dependence of the asymmetry at various collision energies is characterized by the presence of maxima and minima and stems from the angular behavior of the differential cross-sections. At low energies, those features almost reach their maximum by magnitude. The amplitude of features also decreases as the collision energy increases.

The authors express their sincere gratitude to the research assistant Oksana Kudelych for her substantial help in the preparation of the results of this work for the publication.

APPENDIX

Analytical expressions and parameters for the static potential $V_S(r)$ and the total, $\rho(r)$, and spin, $\rho_{sp}(r)$, electron densities for a phosphorus atom

The static potential $V_S(r)$ and the electron densities $\rho(r)$ and $\rho_{sp}(r)$ are calculated using the analytical expressions from work [24]:

$$V_S(r) = -\frac{Z}{r}\left[\sum_{i=1}^{n} A_i \exp(-B_i r) + r\sum_{j=1}^{m} C_j \exp(-D_j r)\right], \quad \text{(A1)}$$

$$\rho_{sp}(r) = \frac{N_{sp}}{4\pi r}\left[\sum_{i=1}^{n} A_i B_i^2 \exp(-B_i r) + \right.$$

$$\left. + \sum_{j=1}^{m} C_j D_j (D_j r - 2)\exp(-D_j r)\right], \quad \text{(A2)}$$

where Z is the nucleus charge of a target atom. In Eq. (A1), the number of terms in the first sum $n = 2$, and $m = 3$ in the second one. The dimensionless parameters A_i equal: $A_1 = -0.09594$ and $A_2 = 1 - A_1$. The parameters B_i, C_j, and D_j have the following values (in terms of a_0^{-1}): $B_1 = 36.3$, $B_2 = 1.56$, $C_1 = -2.5738$, $C_2 = -4.0545$, $C_3 = 1.2231$, $D_1 = 3.5607$, $D_2 = 15.464$ and $D_3 = 7.9518$.

The total electron density is calculated by formula (A2), in which $N_{sp} = Z$, and the parameters n, m, A_i, B_i, C_j, and D_j have the same values as for the calculation of $V_S(r)$ by formula (A1).

The electron density $\rho_\uparrow(r)$ is calculated by formula (A2), where $n = 3$ and $m = 3$. The electron number $N_\uparrow = 9$. The dimensionless parameters A_i equal: $A_1 = -0.07086$, $A_2 = 0.8928$, and $A_3 = 0.18106$. The parameters B_i, C_j, and D_j have the following values (in terms of a_0^{-1}): $B_1 = 37.64$, $B_2 = 12.076$, $B_3 = 1.375$, $C_1 = 1.0565$, $C_2 = -2.0148$, $C_3 = 6.1969$, $D_1 = 1.845$, $D_2 = 16.983$, and $D_3 = 7.6344$.

The electron density $\rho_\downarrow(r)$ is calculated by formula (A2), where $n = 2$ and $m = 3$. The electron number $N_\downarrow = 6$. The dimensionless parameters A_i equal: $A_1 = -0.08497$ and $A_2 = 1.0875$. The parameters B_i, C_j, and D_j have the following values (in terms of a_0^{-1}): $B_1 = 39.1$, $B_2 = 2.036$, $C_1 = -2.846$, $C_2 = -4.7759$, $C_3 = 2.1211$, $D_1 = 3.7272$, $D_2 = 14.535$, and $D_3 = 8.1556$.

1. H.P. Saha and Dong Lin, Phys. Rev. A **56**, 1897 (1997).
2. O. Zatsarinny and S.S. Tayal, J. Phys. B **34**, 3383 (2001).
3. H.P. Saha, Phys. Rev. A **53**, 1553 (1996).
4. D.C. Griffin, M.S. Pindzola, T.W. Gorczyca, and N.R. Badnell, Phys. Rev. A **51**, 2265 (1995).
5. Y. Wang, O. Zatsarinny, K. Bartschat, and J-P. Booth, Phys. Rev. A **87**, 022703 (2013).
6. W.C. Fon, K.A. Berrington, P.G. Burke, and A. Hibbert, J. Phys. B **16**, 307 (1983).
7. M. Kurokawa, M. Kitajima, K. Toyoshima, T. Kishino, T. Odagiri, H. Kato, M. Hoshino, H. Tanaka, and K. Ito, Phys. Rev. A **84**, 062717 (2011).
8. M. Kitajima, M. Kurokawa, T. Kishino, K. Toyoshima, T. Odagiri, H. Kato, K. Anzai, M. Hoshino, H. Tanaka, and K. Ito, Eur. Phys. J. D **66**, 130 (2012).
9. D.G. Thompson, J. Phys. B **4**, 468 (1971).
10. J.C. Slater, *The Self-Consistent Field for Molecules and Solids* (McGraw-Hill, New York, 1974).
11. *Theory of the Inhomogeneous Electron Gas*, edited by S. Lundqvist and N.H. March (Plenum Press, New York, 1983).
12. J.K. O'Connell and N.F. Lane, Phys. Rev. A **27**, 1893 (1983).
13. N.T. Padial and D.W. Norcross, Phys. Rev. A **29**, 1742 (1984)
14. E.Yu. Remeta and V.I. Kelemen, J. Phys. B **43**, 045202 (2010).
15. J. Kessler, Adv. At. Mol. Opt. Phys. **27**, 81 (1991).

16. V.I. Kelemen, M.M. Dovhanych, and E.Yu. Remeta, Ukr. Fiz. Zh. **55**, 1061 (2010).
17. V.I. Kelemen and E.Yu. Remeta, Dopov. Nat. Akad. Nauk Ukr. N 1, 65 (2013).
18. V.A. Fock, *Fundamentals of Quantum Mechanics* (Mir, Moscow, 1978).
19. L.T. Sin Fai Lam, J. Phys. B **15**, 119 (1982).
20. M.S. Rabasović, V.I. Kelemen, S.D. Tošić, D. Šević, M.M. Dovhanych, V. Pejćev, D.M. Filipović, E.Yu. Remeta, and B.P. Marinković, Phys. Rev. A **77**, 062713 (2008).
21. V.I. Kelemen, M.M. Dovhanych, and E.Yu. Remeta, J. Phys. B **41**, 035204 (2008).
22. V.I. Kelemen and E.Yu. Remeta, J. Phys. B **45**, 185202 (2012).
23. V. Kelemen, E. Remeta, and E. Sabad, J. Phys. B **28**, 1527 (1995).
24. T.G. Strand and R.A. Bonham, J. Chem. Phys. **40**, 1686 (1964).
25. V.I. Kelemen, Zh. Tekhn. Fiz. **72**, 13 (2002).
26. A. Zangwill and P. Soven, Phys. Rev. A **121**, 1561 (1980).
27. E.Yu. Remeta and V.I. Kelemen, Dopov. Nat. Akad. Nauk Ukr. N 11, 84 (2011).
28. V. Kelemen and E. Remeta, J. Phys. B **43**, 235204 (2010).
29. V.I. Kelemen, E.P. Sabad, and M.M. Dovhanych, Ukr. Fiz. Zh. **34**, 345 (1989).
30. S.D. Tošić, V.I. Kelemen, D. Šević, V. Pejćev, D.M. Filipović, E.Yu. Remeta, and B.P. Marinković, Nucl. Instrum. Methods B **267**, 283 (2009).
31. F. Calogero, *Variable Phase Approach to Potential Scattering* (Academic Press, New York, 1967).
32. V.V. Babikov, *Phase Function Method in Quantum Mechanics* (Nauka, Moscow, 1988) (in Russian).
33. I. Shimamura, Sci. Papers Inst. Phys. Chem. Res. **82**, 1 (1989).
34. R. Panajotović, D. Filipović, B. Marinković, V. Pejćev, M. Kurepa, and L. Vušković, J. Phys. B **30**, 5877 (1997).
35. P.G. Burke, *Potential Scattering in Atomic Physics* (Plenum Press, New York, 1977).
36. http://ctcp.massey.ac.nz/dipole-polarizabilities
37. A.A. Radtsig and B.M. Smirnov, *Reference Data on Atoms, Molecules, and Ions* (Springer, Berlin, 1986).
38. G.N. Haddad and T.F. O'Malley, Austral. J. Phys. **35**, 35 (1985).
39. R. Szmytkowski, Fizika **22**, 481 (1990).
40. S.K. Srivastava, H. Tanaka, A. Chutjian, and S. Trajmar, Phys. Rev. A **23**, 2156 (1981).

Received 27.06.13.
Translated from Ukrainian by A.I. Voitenko

В.І. Келемен, М.М. Довганич, Є.Ю. Ремета

ПОТЕНЦІАЛЬНЕ РОЗСІЮВАННЯ
ЕЛЕКТРОНА НА АТОМІ ФОСФОРУ

Р е з ю м е

Вперше теоретично досліджено пружне розсіювання електронів на атомах фосфору в області енергій зіткнень 0,01–200 еВ. Інтегральні і диференціальні перерізи розраховано у спін-поляризованому наближенні безпараметричного дійсного оптичного потенціалу. Повна та спінові електронні густини, електростатичний і спінові обмінні і кореляційно-поляризаційні потенціали атома фосфору знайдено у наближенні локальної спінової густини теорії функціонала густини. Застосовуючи різні наближення детально вивчено особливості низькоенергетичної, до 10 еВ, поведінки інтегральних перерізів, які порівняно з даними для сусідніх атомів сірки, хлору та аргону. Спінова обмінна асиметрія розсіювання електронів на атомі фосфору, з напівзаповненою валентною $3p^3$-підоболонкою, досліджена з врахуванням залежності від спіну обмінної та поляризаційної взаємодій.